DIVACANCY ANNEALING IN SILICON MONITORED BY DIFFERENTIAL CALORIMETRY AND INFRARED ABSORPTION SPECTROSCOPY

Sjoerd Roorda,
Groupe de recherche en physique et technology de Couches Minces (GCM) and Département de physique, Université de Montréal, Montréal Québec H3C 3J7 Canada.

Annealing of divacancies in crystalline Si has been characterized by differential scanning and isothermal calorimetry and infrared absorption spectroscopy. Si discs of 0.1 mm thickness have been implanted with 3.4 MeV protons. Scanning calorimetry shows a relatively sharp peak centered around 425 K and a broader feature ranging from 450 to 620 K. The isothermal heat release at 620 K exhibits a single exponential rather than a bimolecular decay. As the annealing progresses, a decrease in infrared absorption at 1.8 μm is observed which is directly related to the annealing of divacancies.

Introduction

Crystal defects in Si and their annealing behaviour have been studied intensively for many years, and several specific defects have been identified by spectroscopic techniques [1]. In spite of their obvious importance, thermodynamic properties of defects have escaped most, but not all [2], of the attention. Specifically, the formation energies of most simple defects in c-Si have never been measured. The only formation energy that is known is that of the monovacancy. It has been deduced from differences in positron lifetime as c-Si approaches its melting point [3].

We have started a study of thermodynamic properties of simple defects in Si, with an emphasis on their non-equilibrium character associated with ion implantation damage. A relatively simple case is the divacacy in Si. Below room temperature, single vacancies and interstitials are already mobile and therefore the divacancy is the simplest defect that can be studied at room temperature. It has a characteristic absorption at 1.8 μm, and therefore is easy to identify, although not so easy to quantify. Initial calorimetry measurements showed a heat release in MeV proton bombarded Si related to the annealing of divacancies [3]. Here, the direct relationship between the loss of infrared absorption upon annealing and the heat release observed in calorimetry is more firmly established. In addition, isothermal calorimetry has been used to observe the kinetics of the divacancy annealing.

Sample preparation and analysis techniques

Crystalline Si discs of 80 - 100 μm thickness were bombarded with 3.4 MeV H^+ ions to a fluence of 1×10^{17} ions/cm^2. Undoped, B-doped, and P-doped Czochralski (Cz) Si were used as well as undoped float-zone (FZ) material. Since more than 99 % of the ions are transmitted for this combination of ion energy and Si thickness, the discs were clamped between two rings which held them at the edge only. During the bombardment, the sample holder was cooled by liquid nitrogen. Furthermore, the ion beam current was kept below 2 μA and rastered over a large 10 cm^2 area, thus limiting the areal power density to less than 0.7 W/cm^2. Nevertheless, the cooling effectiveness of the Si itself was erratic.

After the ion bombardment, the samples were allowed to warm to room temperature, and the bombardment damage was characterized by infrared absorption spectroscopy using a Bomem DA3 Fourier transform infrared spectrometer (FTIR), with a quartz-halogen white-light source, CaF_2 beamsplitter and liquid-nitrogen-cooled InSb detector. Absorption coefficients were calculated with respect to the spectrum of an untreated Si sample, measured under identical conditions. The absorptivities are reported as the product of absorption coefficient and the thickness, αd. Absorption features due to water vapour were prevented by evacuating the instrument. A broad absorption peak, centered around 1.8 μm, indicating the presence of divacancies [5, 6], was clearly evident in most samples. Some discs that did not remain cold enough during the ion bombardment showed no absorption at all, or a reduced absorption. It was found that the divacancy-related absorption was directly proportional to the near-band-edge absorption (at 1.4 μm). This shows that the nature of the damage is comparable in all samples.

Mat. Res. Soc. Symp. Proc. Vol. 316. ©1994 Materials Research Society

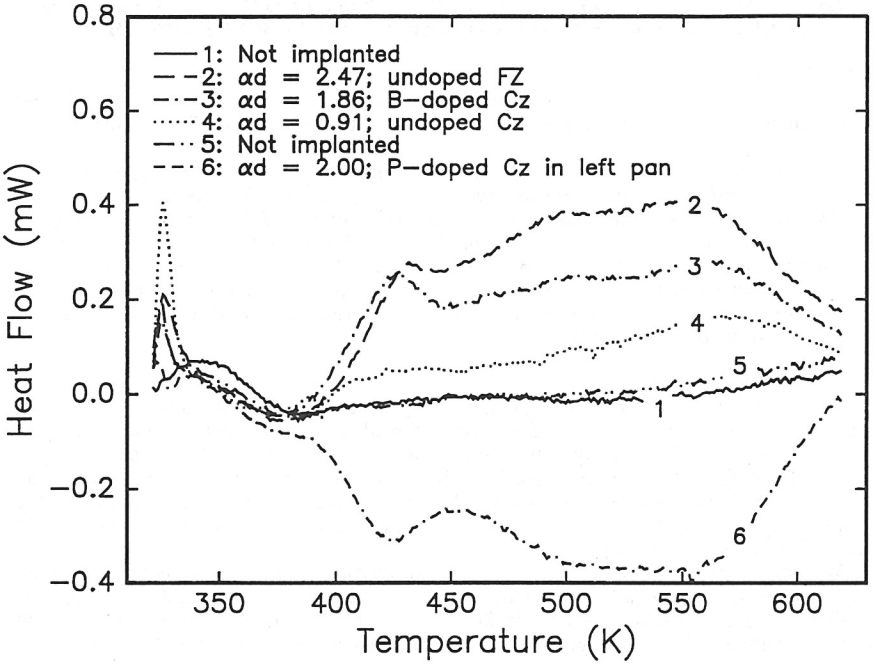

Figure 1. Consecutively measured DSC difference curves. Each curve is the difference between two successive scans. These curves have not been corrected for baseline drift. A positive signal corresponds to a heat release, except for curve 6.

Differential Scanning Calorimetry (DSC) was carried out using a Perkin Elmer DSC2 apparatus. The scanning rate was 40 K/min. and during the scans the sample pans were flushed with dry Ar gas. The samples rested not directly on the sample pans but on graphite spacers. For each measurement, four samples were stacked in one sample pan (on the right) and four identical but non-implanted discs were loaded in the reference pan (on the left). In one case, samples and reference were reversed. Two scans were taken between 320 and 620 K, preceded and followed by several minutes of isothermal measurements. The difference between the first and second scan, corrected for baseline drifts as revealed by the shift of the isothermal signals, represents the heat released by the implanted discs during the first heating run. After the DSC measurements, all discs were again characterized by FTIR to verify that the ion damage has disappeared.

Scanning and isothermal calorimetry

The results from differential scanning calorimetry are shown in Fig. 1. Six curves are shown of the difference between two successive measurements. These sets of scans were numbered according to the order in which they were measured. A positive signal corresponds to a heat release, except for curve no. 6, which was measured with the samples in the left pan and therefore has opposite sign. The curves 1 and 5 were measured on unimplanted material and serve to illustrate the stability and reproducibility of the baseline. Upon reaching the end temperature (620 K), the isothermal difference curves 1 and 5 (not shown) exhibited an almost constant level identical to that of the scanned curves.

For temperatures in excess of 400 K, all curves on ion damaged samples show a clear deviation from the baseline, corresponding to a significant heat release. (The bumps around 350 K are related to the stabilizing of the DSC, and also occur with unimplanted material.)

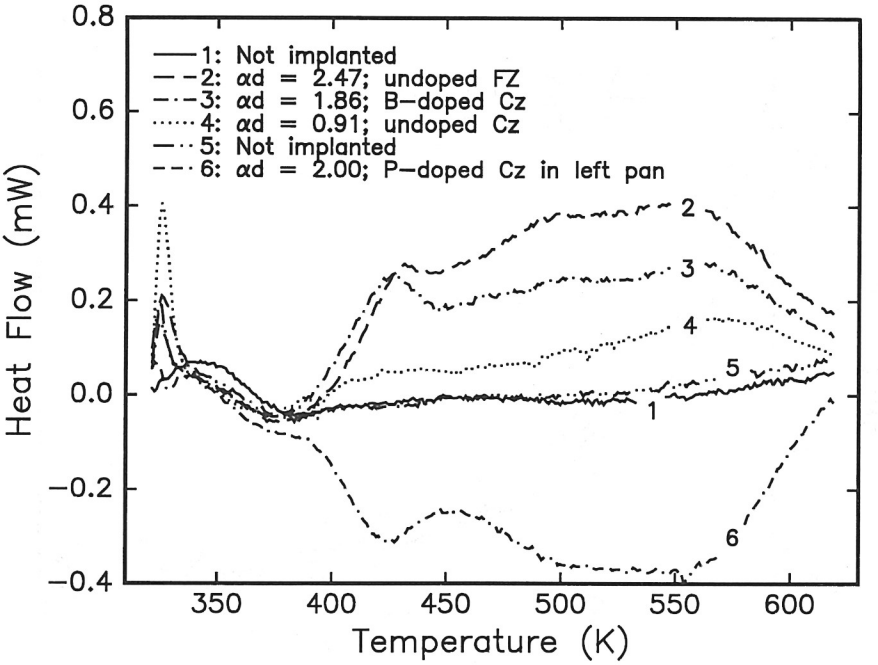

Figure 1. Consecutively measured DSC difference curves. Each curve is the difference between two successive scans. These curves have not been corrected for baseline drift. A positive signal corresponds to a heat release, except for curve 6.

Differential Scanning Calorimetry (DSC) was carried out using a Perkin Elmer DSC2 apparatus. The scanning rate was 40 K/min. and during the scans the sample pans were flushed with dry Ar gas. The samples rested not directly on the sample pans but on graphite spacers. For each measurement, four samples were stacked in one sample pan (on the right) and four identical but non-implanted discs were loaded in the reference pan (on the left). In one case, samples and reference were reversed. Two scans were taken between 320 and 620 K, preceded and followed by several minutes of isothermal measurements. The difference between the first and second scan, corrected for baseline drifts as revealed by the shift of the isothermal signals, represents the heat released by the implanted discs during the first heating run. After the DSC measurements, all discs were again characterized by FTIR to verify that the ion damage has disappeared.

Scanning and isothermal calorimetry

The results from differential scanning calorimetry are shown in Fig. 1. Six curves are shown of the difference between two successive measurements. These sets of scans were numbered according to the order in which they were measured. A positive signal corresponds to a heat release, except for curve no. 6, which was measured with the samples in the left pan and therefore has opposite sign. The curves 1 and 5 were measured on unimplanted material and serve to illustrate the stability and reproducibility of the baseline. Upon reaching the end temperature (620 K), the isothermal difference curves 1 and 5 (not shown) exhibited an almost constant level identical to that of the scanned curves.

For temperatures in excess of 400 K, all curves on ion damaged samples show a clear deviation from the baseline, corresponding to a significant heat release. (The bumps around 350 K are related to the stabilizing of the DSC, and also occur with unimplanted material.)

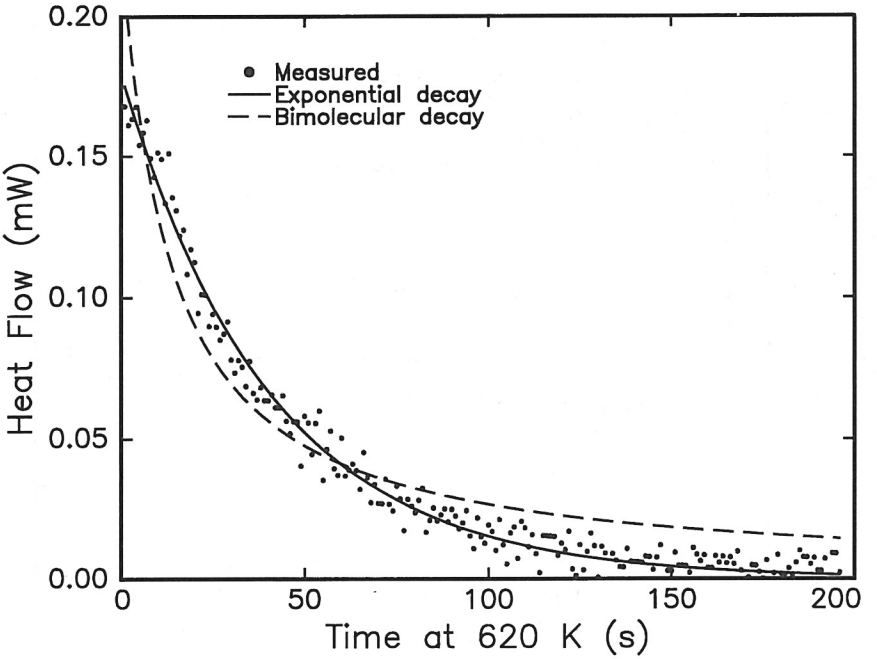

Figure 2. Points: Isothermal heat release following curve 6 in Figure 1. The isotherm has been corrected for baseline drift and the end value has been set to zero. Dashed line: best fit for a bimolecular decay curve. Solid line: best fit for a single exponential decay.

The overall shapes of curves 2, 3, 4, and 6 are identical, with an initial peak centered at 420 K followed by a broad feature ranging from 450 to 600 K. The onset of the first peak appears to be at a slightly lower temperature for the B-doped and P-doped material (curves 3 and 6, respectively) than for the undoped material (curve 2 and 4). An obvious difference between the curves is the magnitude of the heat release. It is found that the total heat release scales with the amount of initial infrared absorption, αd. This is further illustrated in Fig. 3. But first we look at the isothermal behaviour.

An example of an isothermal measurement is shown in Figure 2. The measured curve (shown as points) is the difference between the first and second isotherm, measured upon reaching the end-temperature of the DSC scan with the P-doped Cz samples (curve 6 in Figure 1). A small correction for instrumental instability has been applied (with empty pans, the isothermal difference was found not to be constant, but to decrease slowly and constantly by about 0.015 μW/s), and the estimated signal for infinitely long times has been defined as zero. The decay in heat release reflects the kinetics of the annealing processes and may provide information on their nature.

Two possibilities for a decay mechanism have been evaluated by attempting to fit an appropriate curve to the isothermal data. Assuming a simple exponential decay mechanism, the isothermal calorimetry signal $H(t)$ would decay according to $H(t) = H_0 \cdot \exp(-t/\tau)$, where H_0 signifies the heat release at time 0, and τ the time constant of the decay process. An example of such a mechanism would be the thermally activated break-up of divacancies into single vacancies. The single vacancies thus generated rapidly diffuse and are annihilated either at the surface or at interstitial clusters. Alternatively, the divacancy as a whole might become mobile and combine with other divacancies to form larger vacancy-clusters. Such a mechanism would result in a bimolecular decay, $H(t) = H_0 / (1 + H_0 \cdot k \cdot t)$. Here, k is a

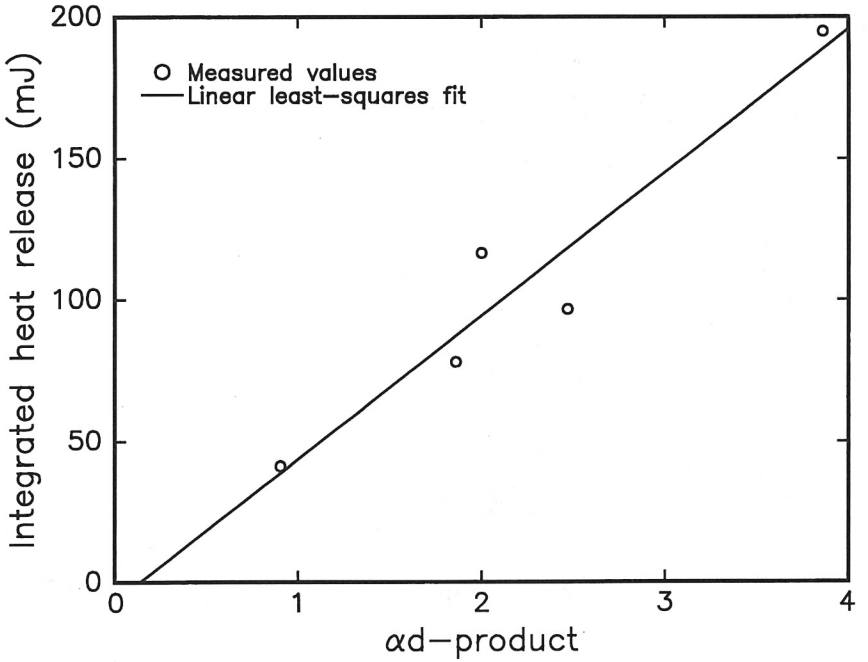

Figure 3. Circles: Relation between initial infrared absorption, measured before DSC, and total heat release. The baseline was obtained from DSC curves for unimplanted material. Before integration, the curves were corrected for baseline drift as revealed by the shift in isotherm end value. Line: linear least-squares fit to the data.

characteristic rate constant. Fitting these expressions gives the drawn and dashed lines shown. Clearly, a single exponential decay gives a much better fit. Not only does the curve follow the points, but the value for H_0 corresponds to the observed heat release at $t = 0$. Assuming for the moment that the heat release is indeed related to divacancy annealing (which will be further corroborated), this would rule out an anneal mechanism whereby the divacancy as a whole becomes mobile.

Correlation between calorimetry and infrared absorption

The absorption band at 1.8 μm observed in ion, neutron, or electron bombarded Si has been identified as an indicator of divacancies [5, 6]. Moreover, the product αd has been reported to be proportional to the divacancy concentration [7]. This allows us to associate the heat release observed in Fig. 1 and 2 with the decay in divacancy concentration. First, the integrated heat release over the entire temperature range can be compared with the initial αd product. (After DSC, the divacancy absorption band had disappeared.) Here, we make use of the fact that some samples were not well cooled during the ion bombardment. Each DSC scan was performed on a stack of four samples, sorted according to αd value. The near-edge absorption, though to indicate the presence of defect clucters, was always found to be directly proportional to the divacancy-absorption. The stacks, therefore, contained different concentrations of divacancies, all other things being equal.

The relation between infrared absorption at 1.8 μm and total heat release is shown in Figure 3. The points represent the measured values. It should be remarked here that the integration of the DSC curves was performed after a correction for baseline shift, determined from the isothermal end value, and for the zero-signal baseline (curves 1 and 5) as shown in

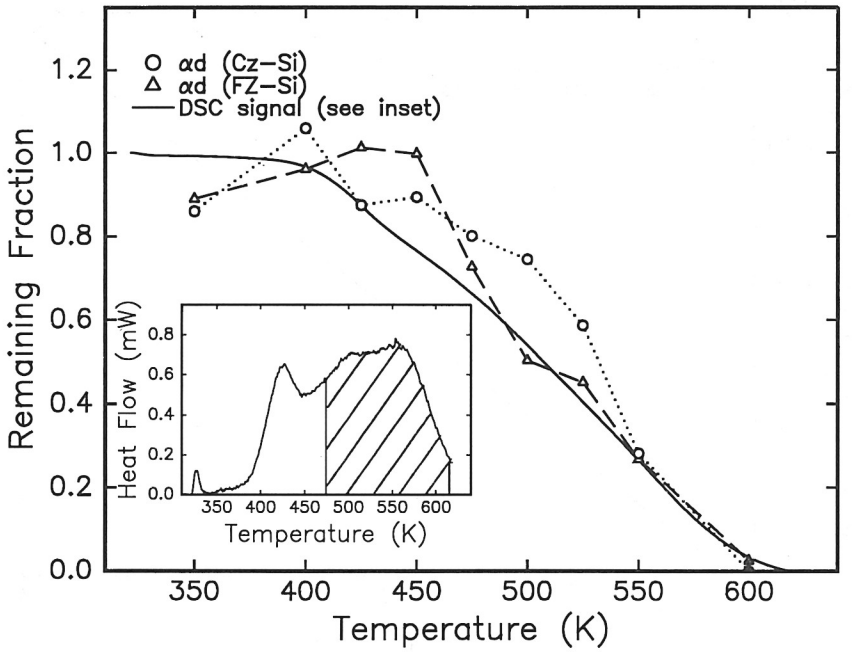

Figure 4. Circles and triangles: Intensity of the 1.8 μm absorption peak after anneal in the calorimeter, normalized to the initial intensity. The dotted and dashed lines are a guide only. Solid line: Heat that remains stored in the material as the DSC measurement progresses. Inset: DSC curve illustrating the calculation of the remaining heat. At 475 K, the remaining heat would be the hatched area divided by the total area under the curve.

Figure 1. (A more detailed explanation of baseline correction procedures has been given elsewhere [8].) The subtraction of zero-signal baselines can be avoided by taking the difference between a curve with the samples in the right pan and one with the samples in the left pan. This was done in one case and resulted in the point in the upper right corner of Figure 3. Passing a linear least squares fit through the points (solid line) gives a good fit which more or less passes through the origin as well. This shows that the integrated heat release is proportional to the infrared absorption αd, which in turn is proportional to the divacancy concentration. This is already a good indication that the heat release observed in Figures 1 and 2 is due to divacancy annealing.

The relation between heat release and infrared absorption was investigated in more detail by studying the anneal behaviour of the infrared absorption band as a function of temperature *under identical conditions as received by the DSC samples*. To this end, several samples were ramp-heated in the DSC instrument using the same heating rate as during the scans (40 K/min). Upon reaching the end temperature, the sample was immediately quenched back to room temperature with a nominal cooling rate of 320 K/min. The absorption was again measured and the ratio in αd before and after the anneal was calculated.

Figure 4 shows the ratio in αd before and after anneal as a function of the anneal temperature. Circles represent undoped Cz-Si and triangles were measured using undoped float-zone material. The dotted lines are a guide to the eye. The ratio reflects the fraction of divacancies remaining in the material after the anneal, whence the ordinate title. The decay over a wide temperature range is similar to the anneal behaviour reported for 15 min.

isochronal annealed neutron bombarded Si [7], except for the apparent increase which can be observed between 400 and 450 K.

In order to compare the infrared absorption band anneal behaviour with the heat release, a curve has been constructed, representing the amount a heat remaining in the material as a function of DSC temperature. The inset in the lower left corner of Figure 4 shows a DSC curve. (In fact this is curve 4 minus curve 6, see Figure 1.) At each temperature, the remaining heat is defined as the area under the curve beginning at the temperature under consideration, divided by the total area under the curve. The inset illustrates this for a temperature of 475 K; the remaining heat would be the hatched area divided by the total area. The curve thus obtained is shown as a solid line in Figure 4; it can be directly compared with the infrared absorption band anneal behaviour.

Comparing the line (remaining heat) with the points (remaining divacancies) it is seen that for temperatures above 500 K, a direct, one-to-one correspondence exists between the two. In the temperature range from 400 to 450 K, a different behaviour seems evident, with a decrease in the remaining heat but an increase in the infrared absorption. This leads to the suggestion that the first DSC peak (observed around 425 K in Figure 1 and the inset of Figure 4) is related to additional *formation* rather than *annihilation* of divacancies (whence the increase in αd). In order to firmly establish this, a more detailed study would be required. The second feature in the DSC curves, the broad heat release signal ranging from 450 to 600 K, (roughly the hatched area in the inset of Figure 4) would then be caused primarily by divacancy annealing.

Conclusion

Divacancies in crystalline Si, generated by passing 3.4 MeV protons through 80 - 100 μm thick c-Si discs, have been studied by differential calorimetry and infrared absorption spectroscopy. Scanning calorimetry reveals a significant heat release in the form of a sharp peak around 425 K and a broad feature ranging from 450 to 620 K. No obvious differences are observed between Cz and float zone material or between P-doped, B-doped, and undoped Si. The DSC curves have been correlated with the anneal behaviour of the 1.8 μm absorption band. This band, which has been identified as a divacancy related absorption feature, shows a steady decrease for anneal temperatures above 450 K and perhaps an increase around 425 K. This would suggest that the initial DSC peak is associated with formation of divacancies, while the broad feature almost certainly is caused by divacancy annealing. The decay of the heat release as a temperature of 620 K is maintained shows a single exponential rather than a bimolecular behaviour. This would exclude an anneal mechanism where the divacancy as a whole becomes mobile and clusters with other divacancies.

Acknowledgments

It is a pleasure to acknowledge the expert assistance of P. Bérichon and R. Gosselin with the operation of the tandem accelerator, J. Graham who set up the infrared spectrometer, and the help of G. Kajrys, L. Cliche, K. Laaziri, and M. Verhaegen with the (lengthy) ion bombardments. I am grateful to F. Spaepen (Harvard University) for making available the DSC instrument and H. Zolla for its calibration. This work is financially supported by the Natural Science and Engineering Research Council of Canada (NSERC) and the Fonds pour la Formation de Chercheurs et l'Aide à la Recherche (FCAR).

References

[1] See, e.g., *Deep Centers in Semiconductors*, ed. S.T. Pantelides (Gordon and Breach, New York 1986).
[2] H. Lim, H.J. von Bardeleben. and J.C. Bourgoin, Phys. Rev. Lett. **58** (1987) 2315.
[3] S. Dannefaer, P. Mascher, and D. Kerr, Phys. Rev. Lett. **56** (1986) 2195.
[4] S. Roorda, G. Kajrys, and J. Graham, Nucl. Instr. and Meth. B, *in press*.
[5] F.L. Vook and H.J. Stein, Rad. Effects **6** (1970) 11.
[6] L.J. Cheng, J.C.Corelli, J.W. Corbett, and G.D. Watkins, Phys. Rev. **152** (1966) 761.
[7] L.J. Cheng and J. Lori, Phys. Rev. **171** (1968) 856.
[8] S. Roorda, W.C. Sinke, J.M. Poate, D.C. Jacobson, S. Dierker, B.S. Dennis, D.J. Eaglesham, F. Spaepen, and P. Fuoss, Phys. Rev. **B44** (1991) 3702.